



# MN1 immunohistochemistry is a sensitive diagnostic biomarker for primitive CNS tumors with *MN1* fusion

Roxane Daniel<sup>1</sup> · Arnault Tauziède-Espariat<sup>2</sup> · Alice Métais<sup>2,3</sup> · Charlotte Berthaud<sup>2</sup> · Noémie Pucelle<sup>2</sup> · Joelle Lacombe<sup>1</sup> · Aurélien Collard<sup>1</sup> · Fabrice Chrétien<sup>1,2</sup> · Pascale Varlet<sup>2,3</sup>

Received: 26 September 2024 / Revised: 7 November 2024 / Accepted: 8 November 2024  
© The Author(s) 2024

**Keywords** MN1 · Astroblastoma · Immunohistochemistry

The diagnosis accuracy of the astroblastoma has improved significantly since its precise histomolecular definition as astroblastoma, *MN1*-altered (AB-*MN1*) in the latest World Health Organization Classification of Central Nervous System tumors (WHO CNS) [6]. This rare, circumscribed astrocytic tumor can now be more easily distinguished from other tumors with radially arranged perivascular cells, such as ependymomas (EPN), pleomorphic xanthoastrocytomas (PXA), and glioblastomas (GBM) or rare gliomas [3, 8, 10–12]. It is associated with a robust methylation signature [originally designated as CNS high-grade neuroepithelial tumors, *MN1*-altered (HGNET-*MN1*)] and characterized by specific fusions affecting the meningioma 1 (*MN1*) gene (22q12.1) and different partners. Recently, some tumors classified by DNA methylation profiling as HGNET-*MN1* were described with *EWSR1::BEND2* [7, 13] or *YAPI::BEND2* fusion [1]. *MN1* is a DNA-binding protein, a transcriptional coregulator, interacting with the BAF complex [9, 14] and mutation has been initially shown in meningiomas [5, 15]. However, there is currently no validated immunohistochemical (IHC) biomarker for *MN1*-altered tumors although *MN1* immunostaining has been tested successfully on *MN1::BEND2* tumors ( $n=9$ ) [4]. The sensitivity and specificity of this biomarker remain to be evaluated.

Our study aimed to evaluate *MN1* IHC on 632 well-annotated, methylation-based, or genetically proven tumor

samples (adult and pediatric) across 56 different histomolecular types/subtypes according to WHO CNS 5 (Table 1).

We applied the antibody anti-*MN1* (polyclonal; rabbit; 1:150 dilution; Proteintech) to 3- $\mu$ m-thick sections of formalin-fixed paraffin-embedded tissue samples, using OMNIS-Automation (Omnis, Santa Clara, California, USA). IHC was performed on whole sections in 466 cases and on tissue microarrays in 166 tumors and was scored as follows: 1 for < 10% of cells with low-intensity nuclear staining; 2 for > 10% with low intensity; and 3 for > 90% of tumor cells with high intensity.

The IHC results, detailed in Table 1, showed strong nuclear labeling in all ( $n=8$ ) but one AB with *MN1::BEND2* fusion (score 2) (Fig. 1B), but this case had been archived for over than 25 years. Astroblastomas *MN1* non-altered (with *EWSR1::BEND2* fusion) ( $n=2/2$ ) were negative (Fig. 1D). The IHC was low in 590 other tumors, including key differential diagnosis of AB (supratentorial (ST) EPN *ZFTA::RELA*-fusion-positive, PXA, mesenchymal GBM IDH-WT) (Fig. 1H, J, L). However, strong expression was also observed in 11 other histomolecular entities ( $n=31$ ) whose positivity was expected (meningioma; ST EPN with *ZFTA::MN1* fusion, neuroepithelial tumors with *PATZ1::MN1* fusion (Fig. 1F, P, R) but also: subependymoma; SEGA; central neurocytoma and others (Fig. 1N, T, V, X, Z). Overall, the sensitivity and specificity of *MN1* IHC in diagnosing primitive CNS tumors with *MN1* fusion were 91.7% and 95.5%, respectively (AB-*MN1* as well as other tumor types with *MN1* fusion).

*MN1* IHC is homogeneously diffuse and intense, simplifying its interpretation. We recommend its routine use to quickly and inexpensively identify potential AB-*MN1* tumors, considering that morphological mimickers are negative. Most *MN1* + tumors have distinct morphological features, making the positive IHC result less impactful

✉ Arnault Tauziède-Espariat  
a.tauziède-espariat@ghu-paris.fr

<sup>1</sup> Université Paris Cité, Paris, France

<sup>2</sup> Department of Neuropathology, GHU Paris, Psychiatry and Neurosciences, Sainte-Anne Hospital, 1, Rue Cabanis, 75014 Paris, France

<sup>3</sup> Institute of Psychiatry and Neurosciences de Paris (IPNP), UMR S1266, INSERM, IMABRAIN, Paris, France

**Table 1** MN1 expression in 632 tumors

Tumor types	MN1 immunostaining, n (%)		
	Negative		Positive
	1 (< 10% of cells, low intensity)	2 (> 10% of cells, low intensity)	3 (> 90% of cells, high intensity)
<b>Adult-type diffuse gliomas</b>			
<b>Glioblastoma, <i>IDH</i>-wildtype</b>			
RTK1 subtype	11/11 (100)	0	0
RTK2 subtype	14/14 (100)	0	0
Mesenchymal subtype	36/41 (88)	5/41 (12)	0
<b>Oligodendroglioma, <i>IDH</i>-mutant and <i>1p/19q</i>-codeleted</b>	12/15 (80)	3/15 (20)	0
<b>Pediatric-type diffuse high-grade gliomas</b>			
Diffuse midline glioma, <i>H3 K27</i> -altered	11/11 (100)	0	0
Diffuse hemispheric glioma, <i>H3.3 G34</i> -mutant	14/14 (100)	0	0
Diffuse pHG, <i>H3</i> -wildtype and <i>IDH</i> -wildtype			
RTK1 subtype	3/3 (100)	0	0
Lynch syndrome	6/6 (100)	0	0
Constitutional mismatch repair deficiency syndrome	9/9 (100)	0	0
RTK2 subtype	1/1 (100)	0	0
<i>MYCN</i> subtype	4/5 (80)	1/5 (20)	0
Li–Fraumeni	1/1 (100)	0	0
Infant-type hemispheric glioma	2/2 (100)	0	0
<b>Meningioma</b>	1/15 (7)	11/15 (73)	<b>3/15 (20)</b>
<b>Circumscribed astrocytic gliomas</b>			
<b>Astroblastoma, <i>MNI</i>-altered*</b>	0/9 (0)	1/9 (11)	<b>8/9 (89)</b>
<b>Astroblastoma, <i>MNI</i> non-altered*</b>	<b>2/2 (100)</b>	0	0
High-grade astrocytoma with piloid features	5/5 (100)	0	0
Pilocytic astrocytoma	17/19 (89)	2/19 (11)	0
<b>Pleomorphic xanthoastrocytoma</b>	12/13 (92)	1/13 (8)	0
<b>Subependymal giant cell astrocytoma</b>	2/10 (20)	4/10 (40)	<b>4/10 (40)</b>
<b>Ependymal tumors</b>			
Myxopapillary ependymoma	9/9 (100)	0	0
Posterior fossa ependymoma, group A	30/30 (100)	0	0
Posterior fossa ependymoma, group B	9/15 (60)	6/15 (40)	0
Spinal ependymoma	22/22 (100)	0	0
Supratentorial ependymoma			
<i>YAPI</i> -fusion-positive	6/6 (100)	0	0
<b><i>ZFTA</i> (non-<i>RELA</i>)-fusion-positive</b>	7/8 (87.5)	1/8 (12.5)	0
<b><i>ZFTA</i>::<i>MNI</i> fusion</b>	0/1 (0)	0	<b>1/1 (100)</b>
<b><i>ZFTA</i>::<i>RELA</i>-fusion-positive</b>	39/40 (97.5)	1/40 (2.5)	0
<b>Subependymoma</b>	5/14 (36)	2/14 (14)	<b>7/14 (50)</b>
Ependymoma-like tumor with <i>PLAGL1</i> fusion	0/2 (0)	2/2 (100)	0
<b>Choroid plexus tumors</b>			
Choroid plexus carcinoma	8/9 (89)	1/9 (11)	0
Choroid plexus papilloma	10/10 (100)	0	0
<b>Embryonal tumors</b>			
AT/RT MYC	7/8 (87.5)	1/8 (12.5)	0
<b>AT/RT SHH</b>	8/13 (62)	3/13 (23)	<b>2/13 (15)</b>
AT/RT TYR	6/6 (100)	0	0
CNS tumor with <i>BCOR</i> internal tandem duplication	7/9 (88)	2/9 (22)	0

**Table 1** (continued)

Tumor types	MN1 immunostaining, n (%)		
	Negative		Positive
	1 (< 10% of cells, low intensity)	2 (> 10% of cells, low intensity)	3 (> 90% of cells, high intensity)
<b>CNS tumor with <i>EP300::BCOR</i> fusion</b>	2/5 (40)	1/5 (20)	<b>2/5 (40)</b>
Embryonal tumor with multilayered rosettes	12/12 (100)	0	0
CNS neuroblastoma, <i>FOXR2</i> -activated	2/2 (100)	0	0
Medulloblastoma, group 3	30/30 (100)	0	0
Medulloblastoma, group 4	30/30 (100)	0	0
Medulloblastoma, <i>SHH</i> -activated and <i>TP53</i> -wildtype	30/30 (100)	0	0
Medulloblastoma, <i>WNT</i> -activated	13/13 (100)	0	0
CNS embryonal tumor with <i>PLAGL1</i> amplification	0/1 (0)	1/1 (100)	0
<b>Pineal tumors</b>			
Pineoblastoma	13/14 (93)	1/14 (7)	0
<b>Mesenchymal tumors</b>			
<b><i>CIC</i>-rearranged sarcoma</b>	4/7 (57)	2/7 (29)	<b>1/7 (14)</b>
Rhabdomyosarcoma	2/2 (100)	0	0
<b>Ewing sarcoma</b>	3/4 (75)	0	<b>1/4 (25)</b>
<b>Intracranial mesenchymal tumor, <i>FET::CREB</i> fusion-positive</b>	2/6 (33)	2/6 (33)	<b>2/6 (33)</b>
Primary intracranial sarcoma, <i>DICER1</i> -mutant	2/2 (100)	0	0
<b>Glioneuronal and neuronal tumors</b>			
Desmoplastic infantile ganglioglioma/desmoplastic infantile astrocytoma	10/10 (100)	0	0
Diffuse leptomeningeal glioneuronal tumor	6/6 (100)	0	0
Dysembryoplastic neuroepithelial tumor	15/15 (100)	0	0
Ganglioglioma	14/14 (100)	0	0
<b>Central neurocytoma</b>	1/8 (12.5)	1/8 (12.5)	<b>6/8 (75)</b>
Papillary glioneuronal tumor	3/3 (100)	0	0
Rosette-forming glioneuronal tumor	7/7 (100)	0	0
Neuroepithelial tumors with <i>PATZ1</i> fusion			
<i>PATZ1::EWSR1</i> fusion	0/1 (0)	1/1 (100)	0
<b><i>PATZ1::MN1</i> fusion</b>	0/2 (0)	0	<b>2/2 (100)</b>

AT/RT, atypical teratoid/rhabdoid tumor; *ZFTA::RELA*, Supratentorial ependymoma *ZFTA::RELA*-fusion-positive. *ZFTA::MN1*, Supratentorial ependymoma *ZFTA* (non-*RELA*)-fusion-positive. *PATZ1::MN1*, Neuroepithelial tumor with *PATZ1* fusion; CNS, central nervous system. Bolded groups represent differential diagnoses, critical information, or unexpected findings

\* All cases of astroblastomas were both confirmed by DNA methylation profiling and RNA sequencing analyses

diagnostically. Interestingly, central neurocytoma, subependymoma and SEGA share a common subependymal location, a similar potential cell of origin (radial glial-like cell) and a MAPkinase/AKT pathway activation (for SEGA and central neurocytoma) [2]. However, information about the function of *MN1* gene and its regulation are currently too limited to understand its causal or non-causal relationship.

Overall, MN1 IHC shows good sensitivity for diagnosing primitive CNS tumors with *MN1* fusion and should be included in routine IHC panels though molecular studies must support the final diagnosis.

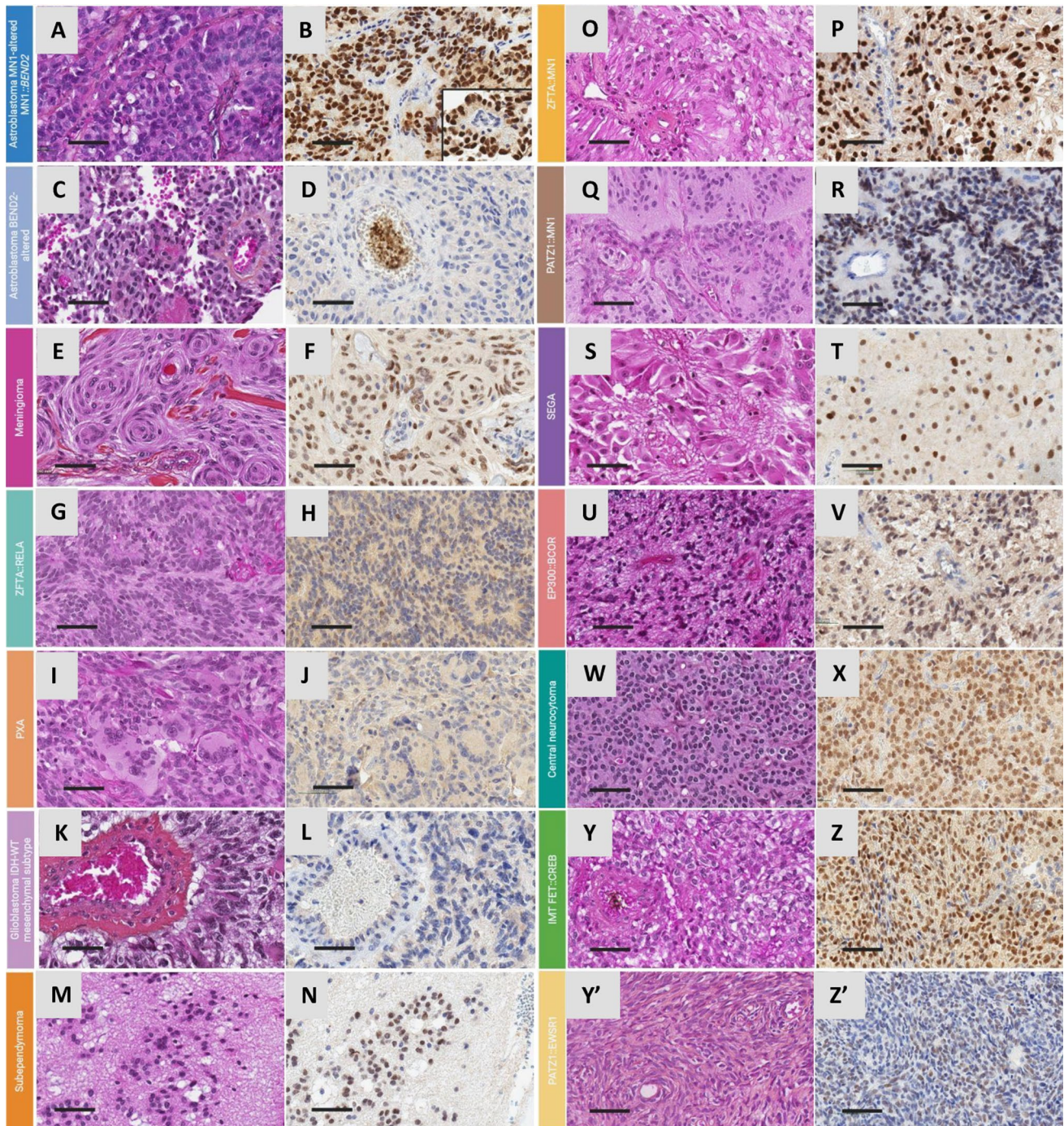


**Fig. 1** Expression of MN1 in primitive CNS tumors, comparing hematoxylin phloxine saffron staining with MN1 IHC. There is diffuse and strong MN1 expression in tumors with *MN1* fusion, particularly astroblastoma, *MN1::BEND2*-fused (B), *ZFTA::MN1* (P), *PATZ1::MN1* (R), as well as meningioma (F) and in unexpected tumors with no *MN1* fusion like SUBEPN (N), SEGA (T),

tumors with *EP300::BCOR* (V), central neurocytoma (X) and IMT *FET::CREB* (Z). Conversely, no MN1 expression is observed in tumors like astroblastoma *BEND2*-altered (D), *ZFTA::RELA* (H), PXA (J), glioblastoma IDH-WT mesenchymal subtype (L) and *PATZ1::EWSR1* (Z'). Scale bars: 50  $\mu$ m

**Author contributions** RD and PV conducted the molecular studies, analysis, interpretation of the IHC data, and drafted the manuscript. ATZ generated the cohort, ATZ and AM helped in the writing of this manuscript. RD, CB, NP, JL, conducted the immunohistochemical techniques. RD and AC conducted the search for blocks.

**Funding** No funding.

**Data availability** No datasets were generated or analysed during the current study.

## Declarations

**Conflict of interest** The authors declare that they have no conflict of interest directly related to the topic of this article.

**Open Access** This article is licensed under a Creative Commons Attribution-NonCommercial-NoDerivatives 4.0 International License, which permits any non-commercial use, sharing, distribution and reproduction in any medium or format, as long as you give appropriate credit to the original author(s) and the source, provide a link to the Creative Commons licence, and indicate if you modified the licensed material. You do not have permission under this licence to share adapted material derived from this article or parts of it. The images or other third party material in this article are included in the article's Creative Commons licence, unless indicated otherwise in a credit line to the material. If material is not included in the article's Creative Commons licence and your intended use is not permitted by statutory regulation or exceeds the permitted use, you will need to obtain permission directly from the copyright holder. To view a copy of this licence, visit <http://creativecommons.org/licenses/by-nc-nd/4.0/>.

## References

- Cuoco JA, Williams S, Klein BJ, Borowicz VM, Ho H, Stump MS et al (2024) Astroblastoma with a novel YAP1::BEND2 fusion: a case report. *J Pediatr Hematol Oncol* 46:e313–e316. <https://doi.org/10.1097/MPH.0000000000002885>
- Lee Y, Chowdhury T, Kim S, Yu HJ, Kim K-M, Kang H et al (2024) Central neurocytoma exhibits radial glial cell signatures with FGFR3 hypomethylation and overexpression. *Exp Mol Med* 56:975–986. <https://doi.org/10.1038/s12276-024-01204-3>
- Lehman NL (2023) Early ependymal tumor with MN1-BEND2 fusion: a mostly cerebral tumor of female children with a good prognosis that is distinct from classical astroblastoma. *J Neurooncol* 161:425–439. <https://doi.org/10.1007/s11060-022-04222-1>
- Lehman NL, Spassky N, Sak M, Webb A, Zumbur CT, Usualieva A et al (2022) Astroblastomas exhibit radial glia stem cell lineages and differential expression of imprinted and X-inactivation escape genes. *Nat Commun* 13:2083. <https://doi.org/10.1038/s41467-022-29302-8>
- Lekanne Deprez RH, Riegman PH, Groen NA, Warringa UL, van Biezen NA, Molijn AC et al (1995) Cloning and characterization of MN1, a gene from chromosome 22q11, which is disrupted by a balanced translocation in a meningioma. *Oncogene* 10:1521–1528
- Louis DN, Perry A, Wesseling P, Brat DJ, Cree IA, Figarella-Branger D et al (2021) The 2021 WHO classification of tumors of the central nervous system: a summary. *Neuro Oncol* 23:1231–1251. <https://doi.org/10.1093/neuonc/noab106>
- Lucas C-HG, Gupta R, Wu J, Shah K, Ravindranathan A, Barreto J et al (2022) EWSR1-BEND2 fusion defines an epigenetically distinct subtype of astroblastoma. *Acta Neuropathol* 143:109–113. <https://doi.org/10.1007/s00401-021-02388-y>
- Mhatre R, Sugur HS, Nandeesh BN, Chickabasaviah Y, Saini J, Santosh V (2019) MN1 rearrangement in astroblastoma: study of eight cases and review of literature. *Brain Tumor Pathol* 36:112–120. <https://doi.org/10.1007/s10014-019-00346-x>
- Riedel SS, Lu C, Xie HM, Nestler K, Vermunt MW, Lenard A et al (2021) Intrinsically disordered Meningioma-1 stabilizes the BAF complex to cause AML. *Mol Cell* 81:2332–2348.e9. <https://doi.org/10.1016/j.molcel.2021.04.014>
- Sari R, Altinoz MA, Ozyar E, Danyeli AE, Elmaci I (2021) A pediatric cerebral tumor with MN1 alteration and pathological features mimicking carcinoma metastasis: may the terminology “high grade neuroepithelial tumor with MN1 alteration” still be relevant? *Childs Nerv Syst* 37:2967–2974. <https://doi.org/10.1007/s00381-021-05289-3>
- Sturm D, Orr BA, Toprak UH, Hovestadt V, Jones DTW, Capper D et al (2016) New brain tumor entities emerge from molecular classification of CNS-PNETs. *Cell* 164:1060–1072. <https://doi.org/10.1016/j.cell.2016.01.015>
- Tauziède-Espariat A, Pagès M, Roux A, Siegfried A, Uro-Coste E, Nicaise Y et al (2019) Pediatric methylation class HGNET-MN1: unresolved issues with terminology and grading. *Acta Neuropathol Commun* 7:176. <https://doi.org/10.1186/s40478-019-0834-z>
- Tsutsui T, Arakawa Y, Makino Y, Kataoka H, Mineharu Y, Naito K et al (2021) Spinal cord astroblastoma with EWSR1-BEND2 fusion classified as HGNET-MN1 by methylation classification: a case report. *Brain Tumor Pathol* 38:283–289. <https://doi.org/10.1007/s10014-021-00412-3>
- van Wely KHM, Molijn AC, Buijs A, Meester-Smoor MA, Aarnoudse AJ, Hellemons A et al (2003) The MN1 oncoprotein synergizes with coactivators RAC3 and p300 in RAR-RXR-mediated transcription. *Oncogene* 22:699–709. <https://doi.org/10.1038/sj.onc.1206124>
- Zhang X, Jia H, Lu Y, Dong C, Hou J, Wang Z et al (2014) Exome sequencing on malignant meningiomas identified mutations in neurofibromatosis type 2 (NF2) and meningioma 1 (MN1) genes. *Discov Med* 18:301–311

**Publisher's Note** Springer Nature remains neutral with regard to jurisdictional claims in published maps and institutional affiliations.